

## THE EFFECT OF SPHEROIDAL GRAPHITE ON FRACTURE PROCESS INITIATION IN CAST IRON

<sup>1</sup>Martin NEVŘELA, <sup>1</sup>Michal WEISZ, <sup>1</sup>Petr SEHNOUTKA, <sup>1</sup>Marek BESEDA

<sup>1</sup>VSB - Technical University of Ostrava, Faculty of Materials Science and Technology, Ostrava, Czech Republic, EU, [martin.nevrela@vsb.cz](mailto:martin.nevrela@vsb.cz)

<https://doi.org/10.37904/metal.2023.4679>

### Abstract

Achieving a balance between strength, toughness and technological properties of cast iron requires knowledge of the relationships between local and macroscopic failure processes. High toughness is conditional upon the substantial dissipation of deformation energy during crack propagation and the initiation of ductile failure. In spheroidal graphite cast iron, toughness depends on the size distribution of these particles, their volume fraction, and the strength of the ferritic matrix/particle phase boundary. The proposed model of fracture surface formation shows how nucleation deformation depends on the local characteristics of the cast iron, graphite particle size, and the strength and energy of the phase boundary. Local fracture deformation during cavity coalescence is most strongly affected by the geometric characteristics of the structure, the spatial distribution of particles, their volume fraction in the matrix, and also the strengthening characteristics of the matrix. The model of fracture surface formation was successfully tested on commercially produced ferritic spheroidal graphite cast iron. The criterion of deformation energy equilibrium was used to predict nucleation deformation and deformation during cavity coalescence. The model can be applied in designing optimized graphite particle size distribution and developing optimized technological parameters for cast iron production.

**Keywords:** Cast iron, deformation energy, crack propagation, ductile failure, spheroidal graphite

### 1. INTRODUCTION

A key requirement for technical applications of spheroidal graphite cast iron is a high level of resistance to the initiation and propagation of fracture processes while also retaining the required levels of strength characteristics. Because plastic deformation is the most important mechanism for stress relaxation at the crack root, cast iron with higher yield strength usually displays higher toughness.

In order to successfully design physical-metallurgical and structural conditions to achieve a balance between strength, toughness and technological properties of cast iron, it is necessary to study the relationships between local and macroscopic failure processes. High toughness is conditional upon the substantial dissipation of deformation energy during crack propagation, enabling the initiation of ductile failure. In spheroidal graphite cast iron designed for wider technical applications, whose structure after heat treatment consists of a basic ferrite matrix with excluded graphite particles, toughness depends primarily on the size distribution of these particles, their volume fraction, the strength of the matrix/particle phase boundary, and the mechanical properties of other structural phases.

Ductile failure of these materials occurs under high plastic deformation of the matrix of cavities nucleated on graphite particles. The typical dimpled topography of the fracture surface, with initiating particles often visible in the dimples, may be a source of further information on the master crack formation mechanism [1]. This mechanism is very strongly affected particularly by the stress state of the specimen. Depending on the specimen's characteristic thickness, a change of plane strain to plane stress at the edges or at crack completion is also reflected in a change of the ductile fracture control mechanism to shear fracture (**Figure 1**).

All the above-mentioned factors combine to influence both the local and total rate of deformation energy dissipation, which also affects the stress/strain field, the size of the plastic zone at the crack tip, the crack propagation rate along the fracture front, and the topographic features of the fracture surface.

By modelling and simulating master crack formation processes in high-energy ductile fracture, it is possible to design appropriate physical-metallurgical and geometric-structural parameters for cast iron in order to achieve the required relationship between strength characteristics and toughness. These methods of designing the structure and properties of structural steels are becoming one of the fundamental tools in new concepts of systematic material development for purposes of specific applications. This paper presents an analysis of ductile fracture initiation conditions in spheroidal graphite cast iron. The aim was to determine the behavioural limit characteristics of spheroidal graphite cast iron that can currently be achieved in view of the given structural state and existing technological possibilities, as well as to propose future ways of determining relationships between microstructure and toughness in spheroidal graphite cast iron.

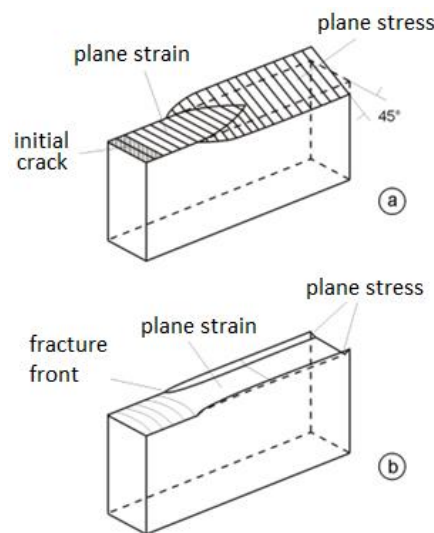


**Figure 1** Change of plane strain to plane stress: a) in thin plates, b) in thick specimens

## 2. MODEL OF CAVITY NUCLEATION IN DUCTILE FRACTURE

Ductile failure of spheroidal graphite cast iron is initiated as a consequence of severe plastic deformation occurring due to decohesion of the matrix and graphite particles. The subsequent stage, involving the growth of cavities nucleated on particles – controlled by the combined effects of the plastic deformation and stress state – leads to an increase in their volume fraction [2, 3]. When the cavity size is comparable with the distance between the particles, the final stage of ductile failure occurs, bringing cavity coalescence [2, 3]. Because all three stages of ductile failure and the processes of fracture surface formation are controlled by a number of different microstructural parameters, it is very difficult to reliably estimate when a localized or macroscopic limit state will occur dependent on loading conditions. Different local conditions for the initiation of plastic deformation, as well as the size distribution and spatial distribution of the graphite particles, mean that the different stages of ductile failure do not occur separately from each other, but increasingly overlap as the plastic deformation increases. The fundamentally different roles played by large and small second phase particles in cavity nucleation have been investigated by Le Roy et al. [2]. Nucleation and cavity growth are suppressed by homogeneous particle distribution as well as by higher hydrostatic content in the stress field. The emergence of localized areas with a substantially higher volume fraction of cavities has a direct influence on the formation of the fracture surface and a substantial effect on its topography and the level of dissipated deformation energy. Severe plastic deformation in the vicinity of the primary cavities nucleates smaller secondary cavities, which increase local dissipation of deformation energy.

Experimental results from studies of ductile failure have been used as a basis for modelling individual stages [4] and also the entire process of high-energy ductile fracture [5]. Efforts to investigate structural changes during plastic deformation growth have always been motivated by the need to identify the microstructural conditions which most effectively prevent the initiation of ductile failure and thus also increase the dissipation of deformation energy during master crack propagation. The first microstructural models led to simple conclusions regarding the dependence of the critical value of nucleation deformation  $\varepsilon_n$  on surface energy at the phase boundary  $\gamma_s$ , elastic constants and size  $d_p$ , and the shape of second phase particles. These models give deformation or stress criteria for cavity nucleation that are dependent on yield strength  $\sigma_0$ , the strength of the matrix/particle phase boundary  $\sigma_n$  and the volume fraction of the graphite particles  $f_v$ . Although nucleation deformation depends on the stress state, it has been found that the phase boundary strength is only very weakly affected by the stress state and the level of plastic deformation [4]. Due to the non-homogeneity of plastic deformation, it is difficult to estimate the maximum stress value at the phase boundary [6]. The original model of phase boundary strength [7] was later elaborated by Brown and Stobbs [8], who estimated phase boundary strength as the sum of local stress  $\sigma_E$  and the yield strength  $\sigma_{0m}$  of the basic matrix, where

$$\sigma_E = 5.4\beta G(2\varepsilon_n b/d_p)^{1.2} \quad (1)$$

and  $\beta$  is a constant,  $\beta = 1/3 - 1/7$ ,  $G$  is the modulus of shear elasticity and  $b$  is the Burgers vector. Besides local stress, the non-homogeneity of deformation on the matrix/particle phase boundary also induces plastic deformation  $\varepsilon_p$  (**Figure 2**).

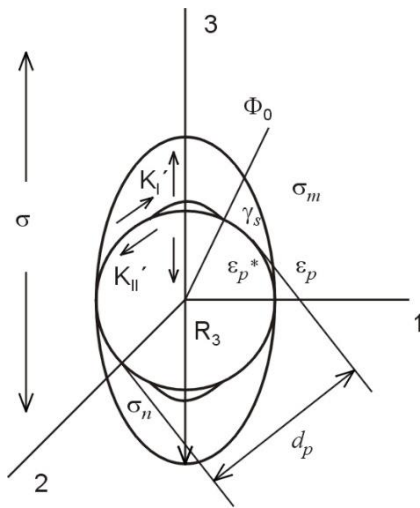


**Figure 2** Stages of cavity nucleation on a spherical particle

Chang and Asaro [9] estimated the maximum stress value at the phase boundary in the form

$$\sigma_i = 2\theta H(d_p/2)^{-0.7} G \varepsilon_p^{0.3} \quad (2)$$

where  $\theta = (7 - 5\nu)/[15(1 - \nu)]$ ,  $\nu$  is the Poisson number and  $H$  is a constant equalling approx.  $4.2 \cdot 10^{-3} \mu\text{m}^{0.7}$  when particle size is below approx.  $d_p = 20 \mu\text{m}$ . Kwon [10] later presented a model in which the phase boundary strength  $\sigma_n$  is the sum of three components: local stress  $\sigma_E$ , stress at the phase boundary  $\sigma_i$ , and the mean value of stress in the matrix  $\bar{\sigma}_m$ .

A less frequently used approach involves evaluating energy at the moment of cavity nucleation on an isolated second phase particle [11] localized in the basic matrix; this approach draws on models of phase boundary strength and local deformation criteria. A precondition for stable cavity nucleation is that the deformation energy released during cavity nucleation  $\Delta E_r(\phi_0, d_p, \varepsilon_p)$  must exceed the work necessary to create a free surface at the matrix/particle phase boundary  $\Delta E_s(\phi_0, d_p, \varepsilon_p)$ ,

$$W = \Delta E_s(\phi_0, d_p, \gamma_s) - \Delta E_r(\phi_0, d_p, \varepsilon_p) \leq 0 \quad (3)$$

where  $\phi_0$  is the angle of particle/matrix decohesion (**Figure 2**). The released deformation energy  $\Delta E_r$  can be approximately expressed in the form

$$\Delta E_r = \frac{\pi d_p^2}{2} \int_0^{\phi_0} G' \sin \phi d\phi + \pi/4 \theta d_p^3 G \varepsilon_p^{*2} + \pi/6 \sigma d_p^3 \varepsilon_p^* \quad (4)$$

where  $\varepsilon_p^*$  is the unreleased part of the total plastic deformation  $\varepsilon_p$  [9],  $\sigma$  is nominal stress, and

$$(5) G' = \frac{1-\nu^2}{E} (K_I^2 + K_{II}^2) \quad (5)$$

is the crack driving force and  $K_I' + K_{II}'$  (**Figure 2**) are the stress intensity factors during cavity nucleation in the vicinity of the particle poles [11].

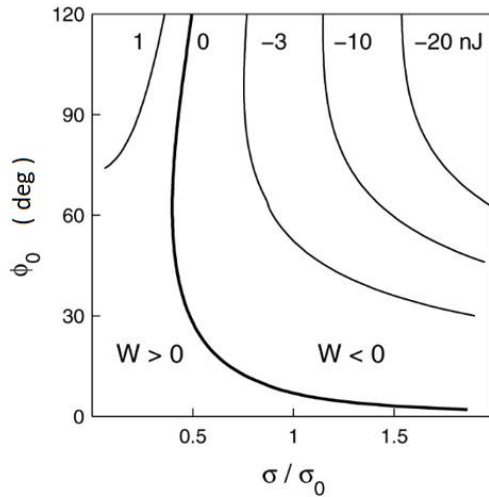


**Figure 3** Dependence of decohesion angle on relative loading for constant values of surface energy and released deformation energy

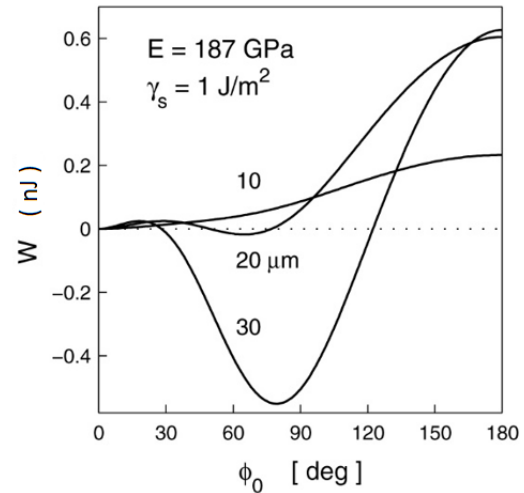


**Figure 4** Difference between surface energy and released deformation energy in decohesion of spherical graphite particles and the matrix dependent on the decohesion angle

In order to apply the energy-based model, nucleation stress conditions must be met. **Figure 3** shows the dependence of the decohesion angle on relative loading  $\sigma/\sigma_0$  for selected constant values of the difference between surface energy and released deformation energy  $W$ . The dependence of plastic deformation  $\varepsilon_p$  on the ratio  $\sigma/\sigma_0$  was determined using the model developed by Rice and Tracey **Chyba! Nenalezen zdroj odkazů..** It is evident from **Figure 3** that the boundary of the stable nucleation area is not monotonous, but there exists a certain critical decohesion angle at which the relative loading necessary for nucleation is minimal. This is even more clearly evident from **Figure 4**, showing the dependence of energy  $W$  on the decohesion angle  $\phi_0$  for selected particle sizes. Nucleation is stable in the area where  $W < 0$ , i.e. for inclusion size  $d_p = 20 \mu\text{m}$  at decohesion angles  $\phi_0 > 45^\circ$ . When  $dW/d\phi_0 = 0$ , this is the moment at which the increased crack size at the particle poles (**Figure 2**) reduces total energy  $W$ . Up to an angle of approx.  $\phi_0 = 20^\circ$ , stable nucleation cannot occur. These examples of numerical approaches to the energy-based model of cavity nucleation appear to be a good basis for other approaches to this process (e.g. statistical approaches). They are undoubtedly useful for an objective estimation of the dependence of cavity volume fraction on loading. Future refinements of the model for cavity nucleation in spheroidal graphite cast iron will primarily require a more precise understanding of the interrelationships between structural and geometric parameters. One promising way of developing new solutions will be to study the effects of spatial distribution and the related effects of the physical-metallurgical and geometric parameters of graphite particles.

### 3. SEVERAL EXPERIMENTAL RESULTS

In order to assess the energy-based model of cavity initiation summarized in the previous section, a study was conducted of commercially produced ferritic cast iron with the following chemical composition:

**Table 1** Chemical composition of the studied cast iron (wt. %)

C	Si	Mn	S	P	Mg	Cu	Ni	Cr
3.35	2.25	0.2	0.006	0.025	0.039	0.06	0.04	0.02

The structure of this cast iron consisted of a basic ferritic matrix with graphite particles of average size 30  $\mu\text{m}$ . The volume fraction of the graphite was estimated at  $f_v = 0.077$ . A tensile test of specimens with circular cross-section averaging 5 mm and gauge length 30 mm showed that the yield strength  $R_{p0.2}$  ranged from 250 to 270 MPa and the elasticity was up to  $A_5 = 18\%$ . The elasticity modulus determined from the linear elastic loading region corresponds with the value  $E=187$  GPa. Pre-deformed specimens were used to prepare specimens for intensive loading to be applied to the central part of their gauge length in order to observe the course of the nucleation stage in the development of ductile failure. **Figure 5** shows the mechanism of gradual cavity nucleation on adjacent graphite particles and the damage caused to the basic matrix by shear plastic deformation. **Figure 6** shows a nucleated cavity with decohesion angle  $\phi_0 = 45 - 55^\circ$  for a total deformation of approx. 5%. This observation corresponds very well with the numerical solution in **Figure 4**.

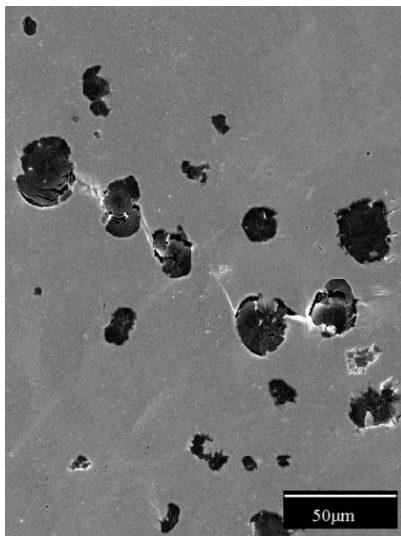


**Figure 5** Mechanism of gradual cavity nucleation on graphite particles and plastic deformation of the matrix

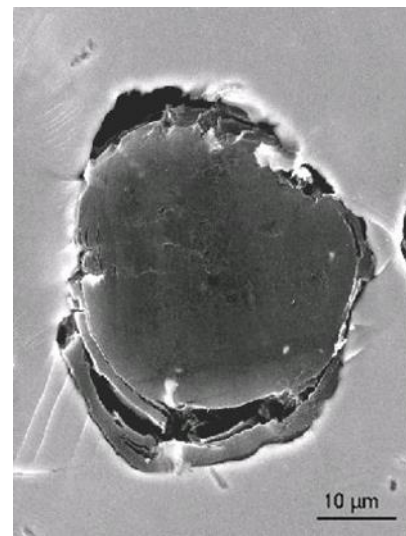


**Figure 6** A cavity nucleated on a graphite particle at approx. 5% plastic deformation

#### 4. CONCLUSION

This analysis of cavity nucleation in the ductile failure of spherical graphite cast iron makes it possible to conduct a local energy assessment of these processes in direct relation to microstructural parameters and external loading conditions. It is evident that stabilization of the nucleation process for a given level of deformation is conditional upon the critical angle of particle/matrix decohesion. The energy equilibrium between the released deformation energy stored in the graphite particle and the energy at the particle/matrix phase boundary can be used as a basis for a number of technological conclusions relevant to the production of these materials with the aim of maximizing the dissipation of deformation energy.

Nucleation deformation is dependent on local characteristics of the cast iron, graphite particle size, the strength and energy of the phase boundary, and also the strengthening characteristics of the matrix. By contrast, local fracture deformation during cavity coalescence is most strongly affected by the geometric characteristics of the structure, the spatial distribution of particles, and their volume fraction in the matrix. The dispersal of material fracture deformation is substantially influenced by the statistical distribution of second phase particle sizes, their spatial distribution, the localized flow of plastic deformation, and local changes in other structural parameters of the cast iron. Although knowledge of the development of plastic deformation in the close vicinity of graphite particles has been used to formulate a number of macroscopic models of master crack propagation during cavity nucleation, growth and coalescence, these models do not include additional stages of the process

or cooperating damage mechanisms. Only a few experimental results are available regarding the development of ductile failure from a three-dimensional perspective, and this will require further study.

## REFERENCES

- [1] HULL, Derek. *Fractography: observing, measuring and interpreting fracture surface topography*. Cambridge: University Press, 1999.
- [2] LE ROY, G., J.D. EMBURY, G. EDWARDS a M.F. ASHBY. A model of ductile fracture based on the nucleation and growth of voids. *Acta Metallurgica*. 1981, vol. 29, no. 8, pp. 1509-1522. Available from: [https://doi.org/10.1016/0001-6160\(81\)90185-1](https://doi.org/10.1016/0001-6160(81)90185-1).
- [3] KWON, D., ASARO, R. J. A study of void nucleation, growth, and coalescence in spheroidized 1518 steel. *Metallurgical Transactions A*. 1990, vol. 21, no. 1, pp. 117-134. Available from: <https://doi.org/doi:10.1007/bf02656430>.
- [4] WILSDORF, H.G.F. The ductile fracture of metals: A microstructural viewpoint. *Materials Science and Engineering*. 1983, vol. 59, no. 1, pp. 1-39. Available from: [https://doi.org/10.1016/0025-5416\(83\)90085-X](https://doi.org/10.1016/0025-5416(83)90085-X).
- [5] LI, Yu-De. An explanation of the relationship of fracture toughness to temperature in the range from upper shelf to first phase transformation. *Engineering Fracture Mechanics*. 1992, vol. 43, no. 2, pp. 305-311. Available from: [https://doi.org/10.1016/0013-7944\(92\)90129-3](https://doi.org/10.1016/0013-7944(92)90129-3).
- [6] QIN, Ying, Er-Feng DU, Yong-Wei LI a Jing-Chen ZHANG. Local Buckling of Steel Plates in Composite Structures under Combined Bending and Compression. *ISIJ International*. 2018, vol. 58, no. 11, pp. 2133-2141. Available from: <https://doi.org/10.2355/isijinternational.ISIJINT-2018-202>.
- [7] ARGON, A. S., J. IM a R. SAFOGLU. Cavity formation from inclusions in ductile fracture. *Metallurgical Transactions A*. 1975, vol. 6, no. 4, pp. 825-837. Available from: <https://doi.org/10.1007/BF02672306>.
- [8] BROWN, L. M. a W. M. STOBBS. The work-hardening of copper-silica v. equilibrium plastic relaxation by secondary dislocations. *Philosophical Magazine*. 1976, vol. 34, no. 3, pp. 351-372. Available from: <https://doi.org/10.1080/14786437608222028>.
- [9] CHANG, Y. W. a R. J. ASARO. Bauschinger effects and work-hardening in spheroidized steels. *Metal Science*. 1978, vol.12.6, pp. 277-284. Available from: <https://doi.org/10.1179/030634578790433756>.
- [10] KWON, D. Interfacial decohesion around spheroidal carbide particles. *Scripta Metallurgica*. 1988, vol. 22, no. 7, pp. 1161-1164. Available from: [https://doi.org/10.1016/S0036-9748\(88\)80123-6](https://doi.org/10.1016/S0036-9748(88)80123-6).
- [11] FISHER, J. R. a J. GURLAND. Void nucleation in spheroidized carbon steels Part 2: Model. *Metal Science*. 1981, vol. 15, no. 5, pp. 193-202. Available from: <https://doi.org/10.1179/030634581790426660>.
- [12] RICE, J.R. a D.M. TRACEY. On the ductile enlargement of voids in triaxial stress fields. *Journal of the Mechanics and Physics of Solids*. 1969, vol. 17, no. 3, pp. 201-217. Available from: [https://doi.org/10.1016/0022-5096\(69\)90033-7](https://doi.org/10.1016/0022-5096(69)90033-7).